Vorticity Alignment and Negative Normal Stresses in Sheared Attractive Emulsions

Alberto Montesi[‡], Alejandro A. Peña[†], and Matteo Pasquali[*]

Department of Chemical Engineering - MS 362, Rice University, 6100 Main St., Houston, TX 77005

(Dated: December 22, 2013)

Attractive emulsions near the colloidal glass transition are investigated by rheometry and optical microscopy under shear. We find that (a) the apparent viscosity η drops with increasing shear rate, then remains approximately constant in a range of shear rates, then continues to decay; (b) the first normal stress difference N_1 transitions sharply from nearly zero to negative in the region of constant shear viscosity; (c) correspondingly, cylindrical flocs form, align along the vorticity and undergo a log-rolling movement. An analysis of the interplay between steric constraints, attractive forces, and composition explains this behavior, which seems universal to several other complex systems.

PACS numbers: 83.80.Iz, 83.50.Ax, 47.55.Dz

Emulsions are relatively stable dispersions of drops of a liquid into another liquid in which the former is partially or totally immiscible. Stability is conferred by other components, usually surfactants or finely divided solids, which adsorb at the liquid/liquid interfaces and retard coalescence and other destabilizing mechanisms.

Emulsions can be regarded as repulsive or attractive, depending of the prevailing interaction forces between drops. In repulsive emulsions, droplets repel each other at any center-to-center distance. On the other hand, attractive emulsions exhibit a potential well at a given distance that exceeds the energy associated to random thermal fluctuations. Consequently, drops in attractive emulsions form flocculates and gel-like structures, whereas droplets in repulsive emulsions do not. This Letter describes for the first time unusual rheological and microstructural features in emulsions under shear, such as alternating changes in the sign of the first normal stress difference with increasing shear rate and formation of domains of drops that align perpendicularly to the direction of shearing. It is shown that these features result from the interplay between composition and attractive forces between droplets. Significant similarities between these trends and those reported for different systems, such as liquid crystalline polymers, colloidal suspensions and polymeric emulsions, are also considered.

Experiments were performed on emulsions of bidistilled water dispersed in a lubricant oil base provided by Exxon Chemicals ($\rho_{\mathsf{oil}} = 871$ kg/m^3, $\eta_{\mathsf{oil}} = 91$ mPa $\cdot$ s at 25 °C). The emulsions were stabilized using the nonionic surfactant SPAN 80 (sorbitan monooleate, Sigma) at a concentration of 5 wt.%. Emulsification was carried out by mixing in 1-inch internal diameter cylindrical plastic container and blending with a two-blade paddle for 10 minutes at 1500 rpm. Droplets in this emulsions form flocs mainly due to micellar depletion attractions, because the concentration of surfactant is well above the critical micellar concentration (< 1 wt.%).

Rheological measurements were carried out in a strain-controlled ARES rheometer using several geometries [1]. Microscopic observations were performed using a customized rheo-optical cell consisting of two parallel glass surfaces, with the upper one fixed to the microscope (Nikon Eclipse E600) and the lower one set on a computer-controlled xyz translation stage (Prior Proscan H101). The glass surfaces were rendered hydrophobic to prevent adhesion and spreading of water drops. All tests were performed at 25.0 ± 0.1 °C.

Figure 1 shows plots of shear viscosity η vs. shear rate $\dot{\gamma}$ for four water-in-oil emulsions with increasing volume fraction of the dispersed (water) phase ϕ. Emulsions for which $\phi = 0.09$, 0.32 and 0.73 exhibited a monotonic viscosity decay characteristic of flocculated emulsions [2]. The shear thinning is related to the progressive breakdown of flocs at low and moderate $\dot{\gamma}$, and to the deformation of drops at high $\dot{\gamma}$. The raise in η with ϕ is a well-known effect caused by an increase in the population of droplets, which leads to higher hydrodynamic interactions among drops and higher resistance to flow. The viscosity of the emulsion with $\phi = 0.58$ first decreased with increasing shear rate, then remained relatively constant and then continued to diminish. This trend has been reported for a few attractive emulsions [3, 4], but it was not explained. Here we explain the microstructural mechanism of the transition in the trend of η, the corresponding anomalous behavior of N_1 and the dependence of these phenomena on the composition of the emulsion.

The rheological behavior of an emulsion made of two Newtonian liquids shifts from viscous to predominantly elastic because of changes in the arrangement of droplets from dilute (uncaged) to caged, to packed, to compressed as the volume fraction of internal phase ϕ grows [5]. At the colloidal glass transition ($\phi = \phi_{\mathsf{g}} \sim 0.58$ [6]), droplets are caged indefinitely by their neighbors and random thermal fluctuations do not disrupt such cages. The volume fraction for close packing of monodisperse

[*]mp@rice.edu, [†]alejandr@rice.edu, [‡]amontesi@rice.edu

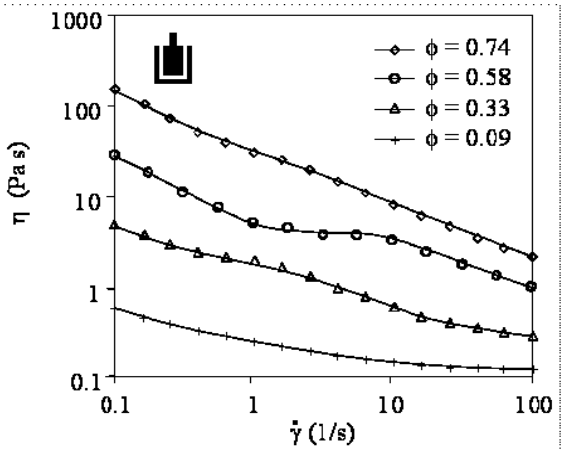

FIG. 1: Steady shear viscosity of water-in-oil attractive emulsions formulated at several water contents. Measurements were performed with the large concentric cylinder geometry.

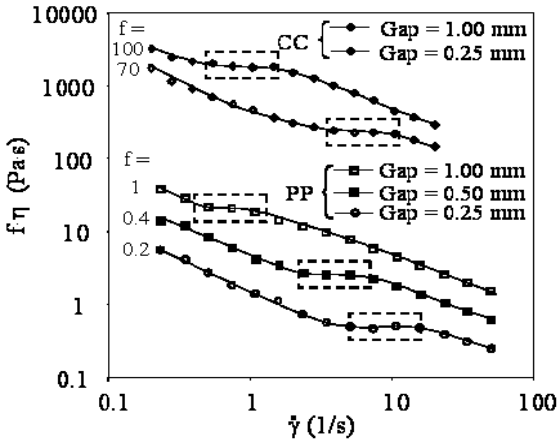

FIG. 2: Effect of the gap thickness on the shear viscosity profile for emulsions with $\phi = 0.58$ for two geometries. The plots have been shifted by a factor f (indicated for each curve) to facilitate interpretation.

hard sphere ϕ_{cp} ranges between 0.64 (random packing) and 0.74 (ordered packing). When $\phi > \phi_{cp}$, the interfaces deform due to compression of drops against drops. Figure 1 shows that a region of constant η occurs for attractive emulsions in the transition from uncaged to compressed, with the effect being more pronounced when $\phi \sim \phi_g$.

Figure 2 shows the shear viscosity of emulsions at $\phi = 0.58$, measured with concentric cylinders (CC) and parallel plates (PP) at several gap thicknesses. A region of constant viscosity was observed in all cases. The range of shear rates in which such phenomenon was observed shifted toward higher $\dot{\gamma}$ as the gap size was reduced. Figure 2 also shows that η remained constant in a wider range of $\dot{\gamma}$ at narrower gap. Noticeably, the shear stress τ in the region of constant η always ranged between 6 and 30 Pa, independently of geometry and gap size. This fact suggests that the onset of a plateau in η is related to changes in the microstructure of the emulsion and that the structural transition involves the formation of domains with characteristic size influenced by the gap size.

Figure 3 shows η and N_1 as a function of the effective $\dot{\gamma}$ between parallel plates for an emulsion with $\phi = 0.58$. N_1 evolved from nearly zero to negative, then from negative to positive as $\dot{\gamma}$ was increased; the sharp transition to negative values of N_1 occurred concomitantly with the plateau in η at each gap size. Experiments with the cone-and-plate geometry, where $\dot{\gamma}$ is uniform across the sample, showed the same effects. We investigated the minimum value of negative normal stresses $N_{1,min}$ as a function of the thickness of the gap between the parallel plates. $N_{1,min}$ was always negative and above the sensitivity of the instrument, and its absolute value grew from 50 to 316 Pa as the gap was reduced from 1.0 to 0.5 mm.

The same trends in N_1 reported in Figure 3 were also observed in tests on emulsions with $\phi = 0.52$ and 0.62, with comparable minimum values of N_1, as shown in Table I. At $\phi = 0.73$ and 0.75 the transition to negative N_1 was much less pronounced and observed in a much narrower region of effective $\dot{\gamma}$. Emulsions with $\phi = 0.32$ did not exhibit any of these features, and $N_1 \simeq 0$ at all $\dot{\gamma}$. These results indicate that the onset of negative N_1

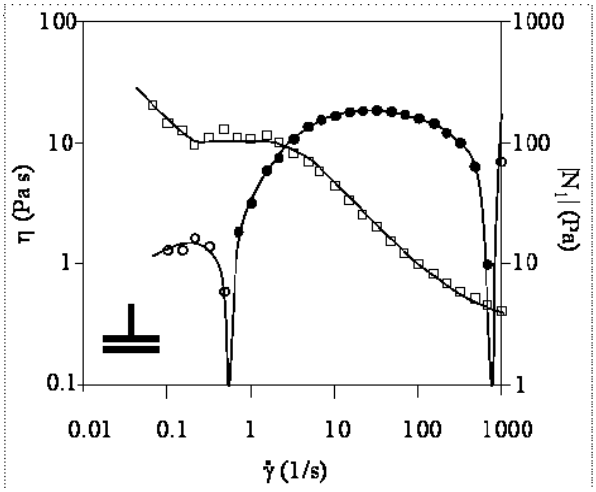

FIG. 3: Steady shear viscosity (squares) and magnitude of the first normal stress difference (circles) vs. shear rate trends for an emulsion with $\phi = 0.58$. Filled circles correspond to negative N_1. Measurements were performed with parallel-plate geometry (gap = 0.65 mm).

ϕ	0.32	0.52	0.58	0.62	0.73	0.75
$N_{1,min}$ **(Pa)**	−24	−238	−210	−223	−159	−50

TABLE I: Minimum N_1 vs. water volume fraction ϕ for pre-sheared emulsions (gap = 0.6 mm). Error in $N_{1,min}$ measurements = ± 30 Pa.

is favored by the caged configuration that droplets adopt near the glass transition. The data reported in Figure 3 and Table I were obtained after pre-shearing the emulsion for 60 s at $\dot{\gamma}$ =100 s^{-1}. This protocol was adopted to improve the reproducibility of N_1 measurements. We observed similar trends for N_1 in emulsions that were not pre-sheared, but the reproducibility of N_1 values was poor. We have also formulated and tested repulsive emulsions that matched the composition, the viscosity ratio of the phases and the interfacial tension of the attractive emulsions studied here. The effects described above were not observed in such repulsive emulsions, thus confirming the key role of attractive forces.

Figure 4 summarizes microscopic observations on the arrangement of droplets under simple shear for an attractive emulsion with $\phi = 0.58$ using the rheo-optical cell described above. Frames (a.1) through (a.4) were taken at increasing shear rates ($\sim$ 0.5, 5, 80 and 120 s^{-1}, respectively). At low $\dot{\gamma}$ (frame (a.1)), the system exhibited a fairly uniform arrangement of droplets. Voids filled with continuous phase (oil) between flocs were present sparsely. When $\dot{\gamma}$ was raised, large flocs disaggregated to form domains surrounded by an increasing number of voids. Speckle-like flocs detached from such domains and tumbled as the emulsion was sheared (frame a.2). At higher $\dot{\gamma}$, the speckles aligned along the direction of vorticity, to form cylindrical flocs that exhibited a "rolling" motion (frame a.3). These cylindrical flocs were still surrounded by large uniform domains. At higher shear rates, the structured configuration of flocs was disrupted (frame a.4) and a nearly uniform arrangement of drops was restored. Frames (b.1) and (b.2) illustrate that the formation of banded flocs in the direction of vorticity was observed independently of the direction in which the emulsion was sheared. In these cases the ordered structure was observed throughout the entire domain. The latter frames were taken with a gap thickness narrower than the one imposed on frame (a.3). The comparison between frames (a.3) and (b.1) suggests that a reduction in the gap led to the formation of finer, more ordered and more evenly distributed band structures. Also, the formation of large voids filled with oil at intermediate shear rates suggests that droplets within the flocs adopted a close-packed configuration as the transition took place. Voids were filled with the oil that came out of the flocs as the local concentration of droplets increased within them. These voids disappeared at high $\dot{\gamma}$ because the shearing disrupted the flocs.

The critical shear rate $\dot{\gamma}_C$ at which the disruption of the ordered structure takes place can be estimated from continuity of shear stress at the outer interface between the flocs and the oil, assuming that the flocs undergo

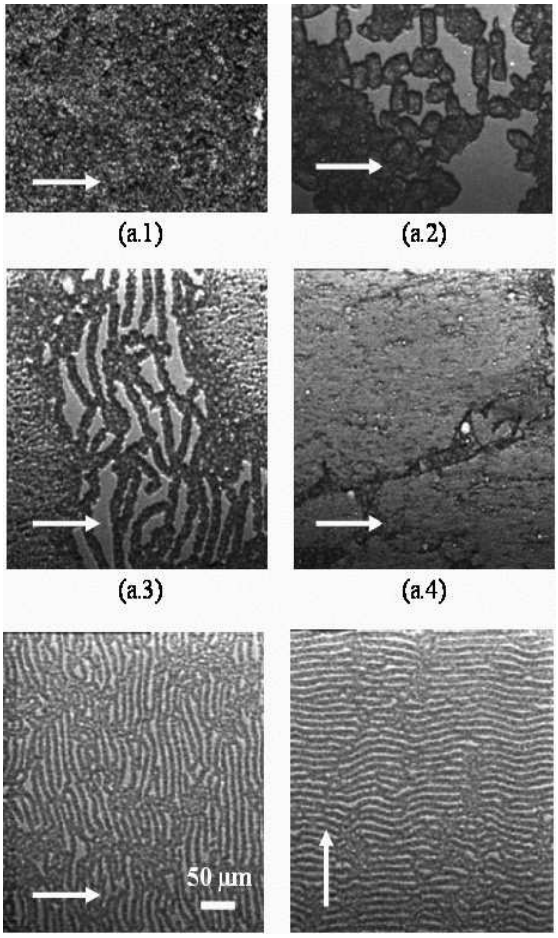

FIG. 4: Microphotographs of emulsions with $\phi = 0.58$ under simple shear for gap thicknesses of (a) 20 μm; (b) 12 μm. Arrows indicate the direction of shear. The reference scale for all frames is inserted in frame (b.1.).

rigid-body rotation with angular velocity ω (Fig. 5.a):

$$\begin{aligned} \tau = \tau_{xy,\mathsf{oil}} &= \tau_{xy,\mathsf{floc}} \\ = \eta_{\mathsf{oil}}\dot{\gamma}_{\mathsf{eff}} &= \eta_{\mathsf{oil}}\left[\frac{\dot{\gamma} - (2r/H)\,\omega}{1-(2r/H)}\right] \end{aligned} \qquad (1)$$

where τ is the shear stress and $\dot{\gamma}_{\mathsf{eff}}$ is the effective shear rate. When $\dot{\gamma} = \dot{\gamma}_C$, τ matches the yield stress of the flocs at the close-packing composition, $\tau^{\mathsf{cp}}_{\mathsf{yield}}$, and $0 \le \omega \le \dot{\gamma}_C$. Therefore, from Eq. 1 we obtain:

$$\dot{\gamma}_{\mathsf{eff}}\left[1-(2r/H)\right] \le \dot{\gamma}_C \le \dot{\gamma}_{\mathsf{eff}};\, \dot{\gamma}_{\mathsf{eff}} = \frac{\tau^{\mathsf{cp}}_{\mathsf{yield}}}{\eta_{\mathsf{oil}}}. \qquad (2)$$

Eq. 2 can be validated with the experiment shown in Fig. 4, frames (a.1-a.4). In this test the cylindrical flocs were disaggregated near $\dot{\gamma} \sim 95$ s^{-1}. From the frame (a.3) in Fig. 4 we obtain $2r/H \sim 0.6$. Also, we measured $\tau^{\mathsf{cp}}_{\mathsf{yield}} \sim 15$ Pa for $\phi_{\mathsf{cp}} \sim 0.74$. With these figures and η_{oil} = 0.091 Pa · s, Eq. 2 renders 68 $s^{-1} < \dot{\gamma}_C < 165$ s^{-1}.

The features described above exhibit striking similarities with the rheological properties of nematic liquid-

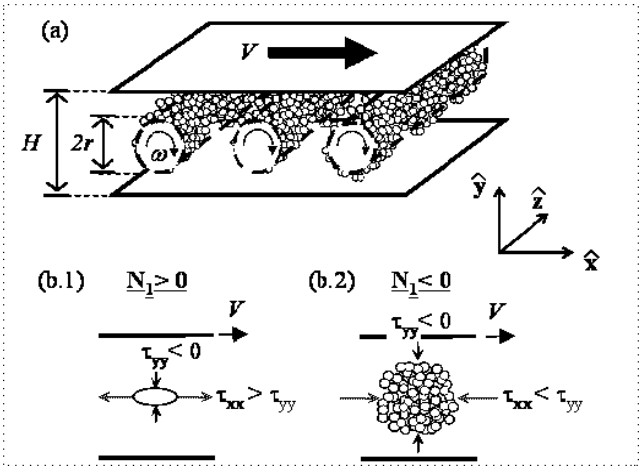

FIG. 5: Schematic representation of (a) the conformation of cylindrical flocs and (b) the stresses in the plane of shear

crystalline polymers (LCP), namely [7, 8, 9]: (a) η vs. $\dot{\gamma}$ plots for LCP solutions commonly exhibit two shear-thinning regions with an intermediate zone of constant viscosity; (b) changes in sign of N_1 first positive to negative, and then negative to positive as $\dot{\gamma}$ is increased are observed for some of these systems; (c) tumbling domains and formation of bands normal to the plane of shear are reported for several lyotropic and thermotropic LCP under shear, sometimes in connection with the above-mentioned trends. Domains of particles that extend along vorticity under shear have also been reported for weakly flocculated magnetic suspensions [10] and thixotropic clay gels [11]. In these latter cases, as well as in the emulsions tested here, attractive forces between particles determined the formation of such domains.

The complex rheological behavior of attractive emulsions reported in this Letter is due to several concomitant factors. First, attractive forces cause the formation of flocs and confer them elasticity. Second, steric constraints impose diameter and ordering of flocs. Third, normal stresses in the shearing plane arise due to the flocs elasticity and make them extend along the vorticity. Elongation of drops along the vorticity was observed in polymeric emulsions [12], and was related to higher normal forces in the dispersed phase relative to the continuous one, which compressed the drops in the shearing plane and caused transverse elongation, in a fashion similar to the phenomenon of rod climbing. The effect is also observed here, with the flocs acting as the viscoelastic dispersed phase. Compression in the $\hat{x}$-$\hat{y}$ shearing plane (Fig. 5.b.2.) leads to a close-packed configuration within the flocs, and to segregation of continuous phase to the surrounding voids. The effect is neither observed in uncaged emulsions because the average distance between drops is large and the flocs are not forced sterically to form compact structures, nor in highly concentrated emulsions because the compressed arrangement of drops inhibits the formation of voids and thus the structural transition. The onset of negative N_1 seems intrinsic to the conformation of flocs along the vorticity. A single drop under simple shear (Figure 5.b.1) is subject to compression in the $\hat{y}$ direction ($\tau_{yy} < 0$) and tension in the $\hat{x}$ direction ($\tau_{xx} > 0$) [13]. Consequently, the drop elongates in the direction of shearing and $N_1 = \tau_{xx} - \tau_{yy} > 0$. On the other hand, the floc is subject to compression in both directions as discussed above (Figure 5.b.2), so $\tau_{xx} < 0$ and $\tau_{yy} < 0$. The growth of the flocs along $\hat{y}$ is restricted by geometry, and growth along $\hat{x}$ is prevented if $\tau_{xx} < \tau_{yy}$ (i.e., $N_1 < 0$). Thus, the flocs can grow in size only along the neutral direction $\hat{z}$. This explains the onset of negative N_1 at the intermediate $\dot{\gamma}$ at which cylindrical flocs form.

The authors wish to acknowledge E. K. Hobbie, K. B. Migler, T. G. Mason, and C. W. Macosko for useful discussions. This work was partially supported by the National Science Foundation (CTS-CAREER-0134389), the Lodieska Stockbrigde Vaughan Fellowship (AAP) and the Rice University Consortium for Processes in Porous Media (G. J. Hirasaki, director).

[1] Rheometrics ARES; cone and plate: plate diameter (diam.) = 25 mm, cone angle = 0.04 rad, gap = 0.051 mm; parallel plates: plate diam. = 25 mm; concentric cylinders: (a) small: cup diam. = 17 mm, bob diam. = 16 mm, bob length = 13 mm; (b) large: cup diam. = 34 mm, bob diam. = 32 mm, bob length = 33 mm.
[2] R. Pal, Chem. Eng. Sci. **52**, 1177 (1997).
[3] R. Pal, Chem. Eng. Sci. **51**, 3299 (1996).
[4] H. Mok Lee, J. Woo Lee, and O. Ok Park, J. Colloid Interface Sci. **185**, 297 (1997).
[5] T. G. Mason, Curr. Opin. Colloid Interface Sci. **4**, 231 (1999).
[6] T. G. Mason, M. D. Lacasse, G. Grest, D. Levine, and J. Bibette, Phys. Rev. E **56**, 3150 (1997).
[7] G. Marrucci, *Liquid crystallinity in polymers: principles and fundamental properties* (VCH Publishers, New York, 1991), chap. 11.
[8] G. Kiss and R. S. Porter, *Mechanical and thermophysical properties of polymer liquid crystals* (Chapman & Hall, London, 1998), chap. 11.
[9] R. G. Larson, *The Structure and Rheology of Complex Fluids* (Oxford University Press, New York, 1999).
[10] R. C. Navarrete, V. E. Le, G. G. Glasrud, C. W. Macosko, and L. E. Scriven, *Theoretical and applied rheology* (Elsevier, Amsterdam, 1992), p. 625.
[11] F. Pignon, A. Magnin, and J. M. Piau, Phys. Rev. Lett. **79**, 4689 (1997).
[12] E. K. Hobbie and K. B. Migler, Phys. Rev. Lett. **82**, 5393 (1999).
[13] W. R. Schowalter, *Mechanics of Non-Newtonian Fluids* (Pergamon Press, Oxford, 1978).